Int. J. Electrochem. Sci., 15 **(2020)** 7370 – 7380, doi: 10.20964/2020.08.81

International Journal of
ELECTROCHEMICAL
SCIENCE
www.electrochemsci.org

The Kinetic Parameters Derived Based on Transient Current Changes in Paired Electrolysis at Rotating Disc Electrode for an E' Reaction in a Highly Concentrated Electrolyte

G. Muthuraman[1,£], *P. Silambarasan*[1,£], *W.G. Shim*[2,£], *and I. S. Moon*[1,*]

[1] Department of Chemical Engineering, Sunchon National University, 255-Jungang ro, Suncheon-si, Jeollanam-do, 57922, South Korea,
[2] Department of Polymer Science and Engineering
[£]These authors are equally contributed to this work.
[*]E-mail: ismoon@sunchon.ac.kr

Received: 7 November 2019 / *Accepted:* 5 June 2020 / *Published:* 10 July 2020

A theoretical model validation with an evaluation of the kinetic parameters for variations in the bulk concentration in an E' reaction with quasi-reversible reduction in a high concentration electrolyte is still desirable. A transient current approach was developed using a collocation model to validate the variations of the $[Co(II)(CN)_5]^{3-}$ (Co(II)) reduction current using a rotating disc electrode (RDE) during $[Co(I)(CN)_5]^{4-}$ (Co(I)) concentration variations in a bulk solution by flow electrolysis. The experimentally observed transient currents, at either different rotation speeds or temperatures, were well matched, highlighting the suitability of the developed transient model. The kinetic parameters, such as the transfer coefficient (α), diffusion layer thickness (δ), heterogeneous electron transfer (k_s), mass transfer coefficient in the form of dynamic diffusivity (D), and energy of activation (E_a), were derived for the Co(II) reduction at the high concentrated electrolyte. The heterogeneous electron transfer region identified showed that Co(II) reduction follows quasi-reversible reduction in high concentration electrolyte media.

Keywords: Collocation model, transient current, theoretical validation, quasi-reversible E'reaction.

1. INTRODUCTION

Membrane-divided paired electrolysis plays a key role in many fields, such as redox flow batteries, fuel cells, and mediator generation, either heterogeneous or homogeneous, and electro-organic synthesis [1-4]. In all fields, high concentration electrolytes have been adopted to stabilize the reduced/oxidized species [5,6] in homogeneous solution. In all vanadium redox flow batteries, 4-5 M H_2SO_4 has been used in most studies [7,8]. Ag(II) was stabilized in highly concentrated acids through

long-lived free radicals [9], and used as a homogeneous mediator ion for the air-pollutant removal process in electro-scrubbing [10]. In a similar manner, a high concentration alkaline medium has been used to stabilize electrogenerated Co(I) [11] and applied as a homogeneous reductive mediator ion in the dehalogenation of air pollutants [12]. Electron transfer and diffusion phenomena parameters can vary in high concentration electrolytes [13]. Although the developed theoretical models did not focus on the concentration of the electrolyte in kinetic parameter derivation [14], the high concentration electrolyte can influenced the derivation of the kinetic parameters. Therefore, kinetic parameters, such as the heterogeneous electron transfer rate (k_s), transfer coefficient (α), and diffusion layer thickness (δ), in a high concentration electrolyte under flow conditions is still desirable. Many theoretical models for an E' reaction considered the ion current at the electrode surface or interface only [15-17], which is measured as the steady state current. Although a few theoretical models considered the ion current in the bulk solution during bulk electrolysis with a definite diffusion layer thickness [18], which is measured as the non-steady state current, the developed transient current change model also needs to be validated experimentally.

In the present investigation, $[Co(II)(CN)_5]^{3-}$ (Co(II)) in a 10 M KOH solution was used as the model compound for the transient current measurements by a rotating disc electrode during the electrolytic generation of $[Co(I)(CN)_5]^{4-}$ (Co(I)). A GC (glassy carbon) electrode was used at different RPM (revolutions per minute) to measure the current of Co(II) reduction as a function of the electrolysis time and temperature. After validating the experimentally observed transient current variations using an orthogonal collocation (OC) model with modified conditions, the heterogeneous rate (k_s), transfer coefficient (α), diffusion layer thickness (δ), and energy of activation (E_a) were derived.

2. MATHEMATICAL MODEL

The mathematical model is derived based on the following known equations for the diffusion and convection. The concentration changes for each electroactive species at a particular point can be described using the one dimensional convection-diffusion equation [19]:

$$\frac{\partial c_i}{\partial t} = \mathrm{D}\frac{\partial^2 c_i}{\partial z^2} - V_z\frac{\partial c_i}{\partial z} \qquad (i = A, B) \tag{1}$$

where c (mol cm^{-3}), D ($cm^2\ s^{-1}$), and V_z ($cm^2\ s^{-1}$) are the concentration, corresponding diffusion coefficients, and axial velocity of fluid at the electrode surface, respectively. Here, the two electroactive species were assumed to have identical diffusion coefficients. In addition, the V_z is a function of the kinematic viscosity ($\upsilon, \mathrm{cm}\ s^{-1}$) and the rotational velocity (ω, s^{-1}) that was expressed using the Von Karman and Cochran equation [19] and can be written as follows:

$$V_z = -0.51023\upsilon^{-\frac{1}{2}}\omega^{\frac{3}{2}}z^2 \tag{2}$$

In addition, the concentration changes in the bulk can be described using the following form [18]:

$$\frac{\partial c_{i,bulk}}{\partial t} = -D\left(\frac{A}{V-A\delta}\right)\frac{\partial c_{i,bulk}}{\partial z}\Big|_{z=\delta} \qquad (i = A, B) \tag{3}$$

where V (cm^3), A (cm^2), and δ (cm) are the total electrolyte volume, electrode area, and thickness, respectively. The initial and boundary conditions considering a simple redox reaction ($A+ne^- \leftrightarrow B$) and a quasi-reversible electron transfer (or the Butler-Volmer equation) can be written as [18,14]

$$t = 0, \;\; 0 \le z \le \delta: \;\; C_A = C_{A0}, \;\; C_B = 0 \tag{4}$$

$$t = 0, \;\; \delta \le z \le \infty: \; C_{A,bulk} = C_{A0}, \;\; C_{B,bulk} = 0 \tag{5}$$

$$z = 0: \;\; \frac{\partial C_A}{\partial z} = -\frac{\partial C_B}{\partial z} \tag{6}$$

$$D\frac{\partial C_A}{\partial z} = k_s\left[exp\left\{-\alpha(E-E^0)\left(\frac{F}{RT}\right)\right\}C_{A0} - exp\left\{(1-\alpha)(E-E^0)\left(\frac{F}{RT}\right)\right\}C_{B0}\right] \tag{7}$$

where k_s (cm s^{-1}), α, E^0 (mV), F, R, and T are the standard heterogeneous rate constant, charge transfer coefficient, standard reduction potential of the electrode, Faraday constant, universal gas constant, and temperature in Kelvin, respectively.

$$z = \delta: \;\; C_A = C_{A,bulk}\,, C_B = C_{B,bulk} \tag{8}$$

In this study, the orthogonal collocation method (OCM) was used to solve the above set of the governing rotating disk electrode equations. The partial differential equations were first discretized into a set of ordinary differential equations (ODEs) by applying the OCM. These discretized ODEs were then solved efficiently using the variable coefficients ordinary differential equation (DVODE) solver [18, 20-22]. The Nelder-Mead simplex method [23] was employed to determine the optimized values of the key parameters, including the diffusion coefficient (D), standard heterogeneous rate constant (k_s), transfer coefficient (α), and thickness (δ).

3. EXPERIMENTAL

3.1. Materials

KOH (99.8%) and $KMnO_4$ were obtained from Junsei Chemical Co., Ltd. (Japan). Sulfuric acid (95%) was supplied by Samchun Chemical Co., Ltd. (South Korea). The silver mesh was purchased from 4scientific, USA. The Ti mesh and Pt-coated Ti mesh electrodes were purchased from Wesco Electrodes and Systems (South Korea) for electrolysis. Tubular Ag, Ti, and carbon electrodes, 6 mm in diameter, were purchased from CJ engineering, Korea for the tubular flow cell sensor experiments. All solutions were prepared using reverse osmosis purified water (Human Power III plus, South Korea) with a resistivity of 18 M.cm. The $[Co(II)(CN)_5]^{3-}$ was synthesized using a reported procedure [24].

3.2. In-situ RDE analysis with paired electrolytic process

A three neck round bottom flask as catholyte tank attached to a Nafion324 membrane-divided electrolysis cell was used for the in-situ measurements of the $[Co(II)(CN)_5]^{3-}$ during electrolytic reduction. Among the three necks, a glassy carbon (from PAR, U.S.A) RDE was used in one neck with a rotator from Prinstan applied research (Model 616A, U.S.A). The other two necks were used for the reference (Ag_{quasi} or Ag/AgCl) and counter Ti electrodes. All three electrodes were connected to a Potentiostat/Galvanostat (PAR- VersaSTAT 3) for the transient current measurements using CV or linear sweep voltammetry (LSV) analysis.

The paired electrolysis experiments were carried out, as reported elsewhere [Ref.12]. In brief, A 0.25 L solution of 5 mol/L sulfuric acid and 0.25 L of $[Co(II)(CN)_5]^{3-}$ (10 mmol/L) in 10 M KOH were placed in separate anolyte and catholyte tanks, respectively. The anolyte and catholyte solutions were circulated continuously through the anode and cathode compartments of the electrochemical cell at constant flow rates (2 L min^{-1}) using magnetic pumps (Pan World Co., Ltd, Taiwan) through a narrow gap in the divided cell (divided by Nafion@324 membrane). The active (Co(I)) electron mediator was generated galvanostatically by applying a constant current density of 25 mA cm^{-2} using a DC power supply **(**Korea Switching Instruments). The effective surface area of each electrode exposed to the solution was 4 cm^2. Mesh-type Cu and Pt-coated Ti electrodes were used as the anode and cathode, respectively. All measurements were taken in triplicate at 20° C.

4. RESULTS AND DISCUSSION

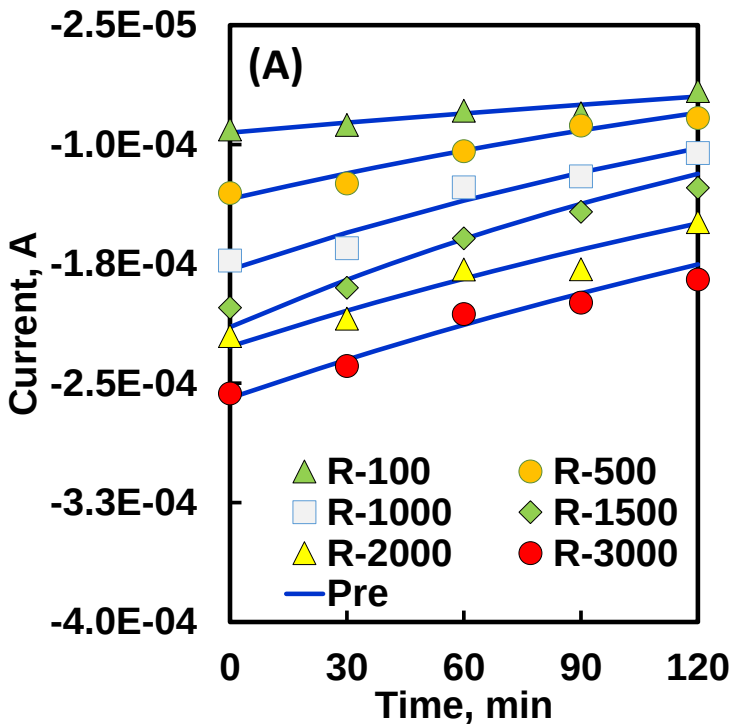

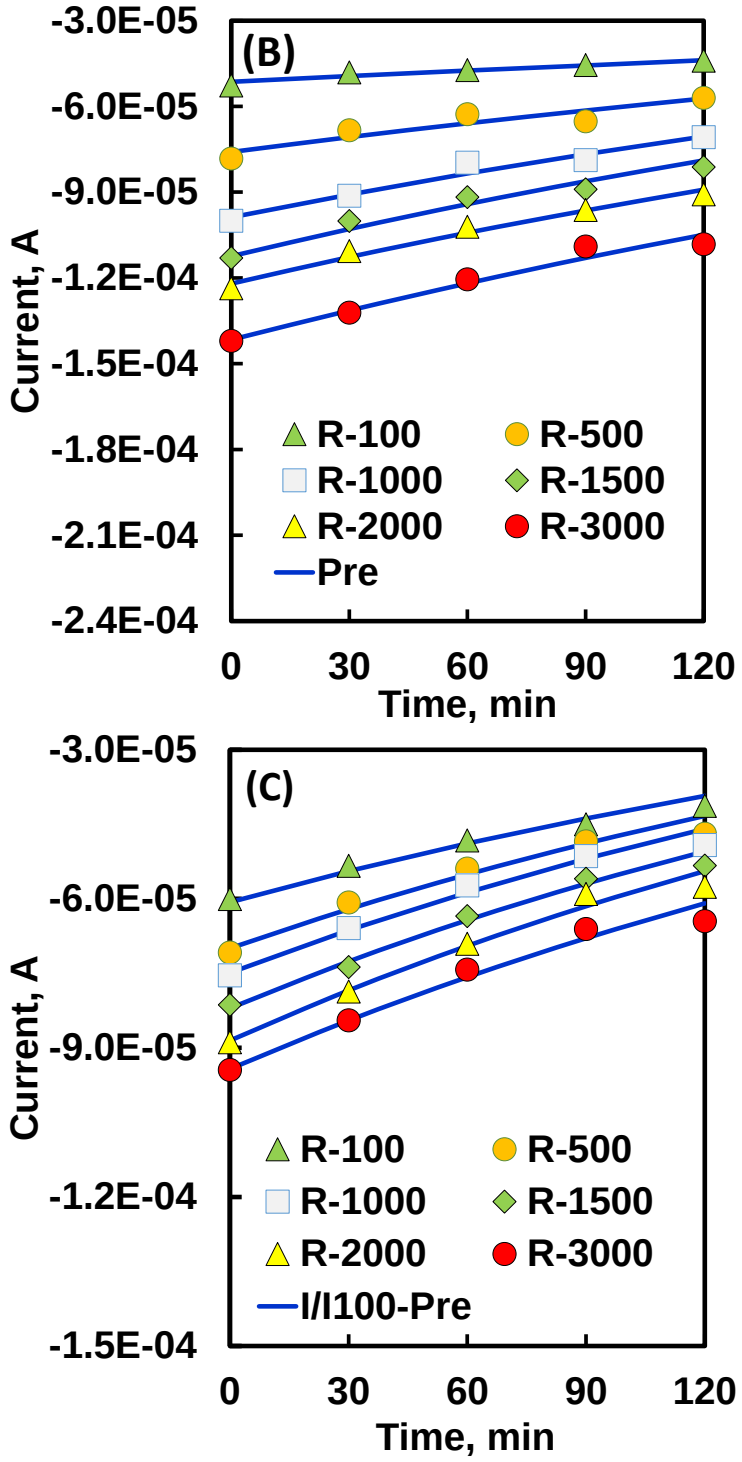

Figure 1. Experimentally observed transient current (symbols) and predicted current (line) for $[Co(II)(CN)_5]^{3-}$ reduction in a 10 M KOH medium with different rotation speeds (mentioned in the figure (R-100 to R-3000)) at (A) 0 °C, (B) 10 °C, (C) 25 °C. Scan rate – 20 mV/s.

Fig.1 shows the reduction current (*i*), which was measured by in-situ LSV at a given time, of $[Co(II)(CN)_5]^{3-}$ (Co(II)) during electrolysis or $[Co(I)(CN)_5]^{4-}$ (Co(I)) concentration variations with

different rotation rates (points (R-100 to R-3000)) along with the values predicted (solid line (Pre)) using the developed model. Fig.1A shows the *i* variation of Co(II) reduction at 0 °C with different electrolysis times, where a non-steady state current or transient current with electrolysis time was found, particularly at low rotation speeds (100 RPM). The transient current difference was 2.26×10^{-5} A with the variations of the Co(I) concentration. At the same time, a larger transient current difference (0.86×10^{-4} A) was found at a high rotation speed (3000 RPM).

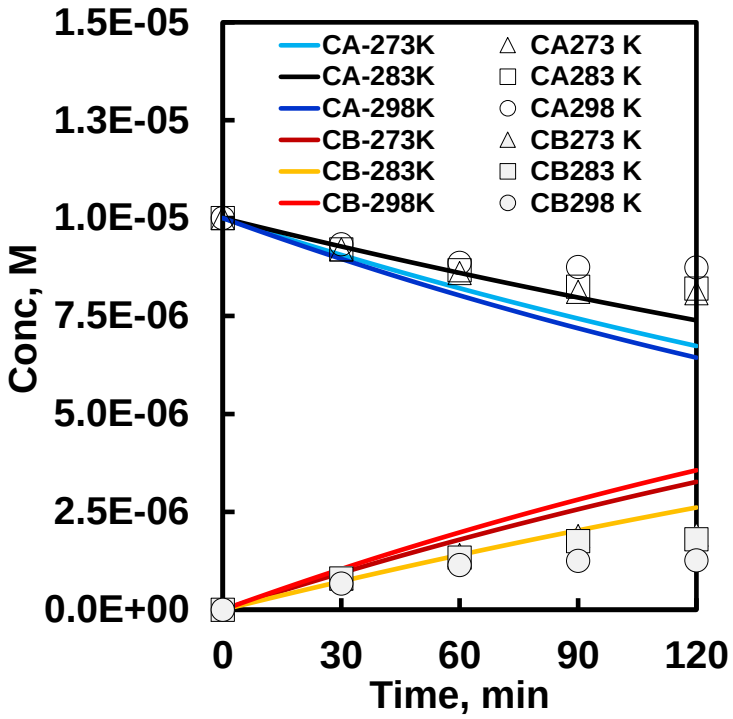

Figure 2. Experimentally observed concentration (symbols) and predicted concentration (Eqs. 1&3) of $[Co(I)(CN)_5]^{4-}$ (Co(I), CB) from 10 mM $[Co(II)(CN)_5]^{3-}$ (Co(II), CA) in 10 M KOH during electrolysis at different temperatures (mentioned in the figure). Conditions: rotation speed = 1500 RPM and scan rate = 20 mV/s.

The predicted transient currents were in good agreement with the experimental values , validating the developed non-steady state model. When the reaction temperature was increased to 10 °C, the overall Co(II) reduction current and transient current difference decreased (0.75×10^{-5} A at 100 RPM and 0.37×10^{-4}A at 3000 RPM) (Fig.1B). Further increases in reaction temperature to 25 °C (Fig.1C), resulted in a larger decrease in the overall Co(II) reduction current, but the difference in the transient current was almost maintained (2.14×10^{-5} A at 100 RPM and 3.33×10^{-5} A at 3000 RPM). The Co(II) reduction current decreased with increasing temperature, which explains the decrease in stability of the active cobalt species with increasing temperature [25]. The Co(II) reduction current, predicted reduction current, and transient current varied with temperature.

Fig.2 shows the potentiometrically derived solution concentration during the electrolytic reduction of Co(II) at different temperatures (Fig.2 symbols) for different electrolysis times. The Co(I) concentration increased with increasing electrolysis time to 0.19 mM for 0 °C (Fig.2 points CA), which

decreased with increasing temperature to 0.12 mM (Fig.2 points CA-298K). In contrast, the Co(II) concentration decreased with increasing electrolysis time (Fig.2 points CB).

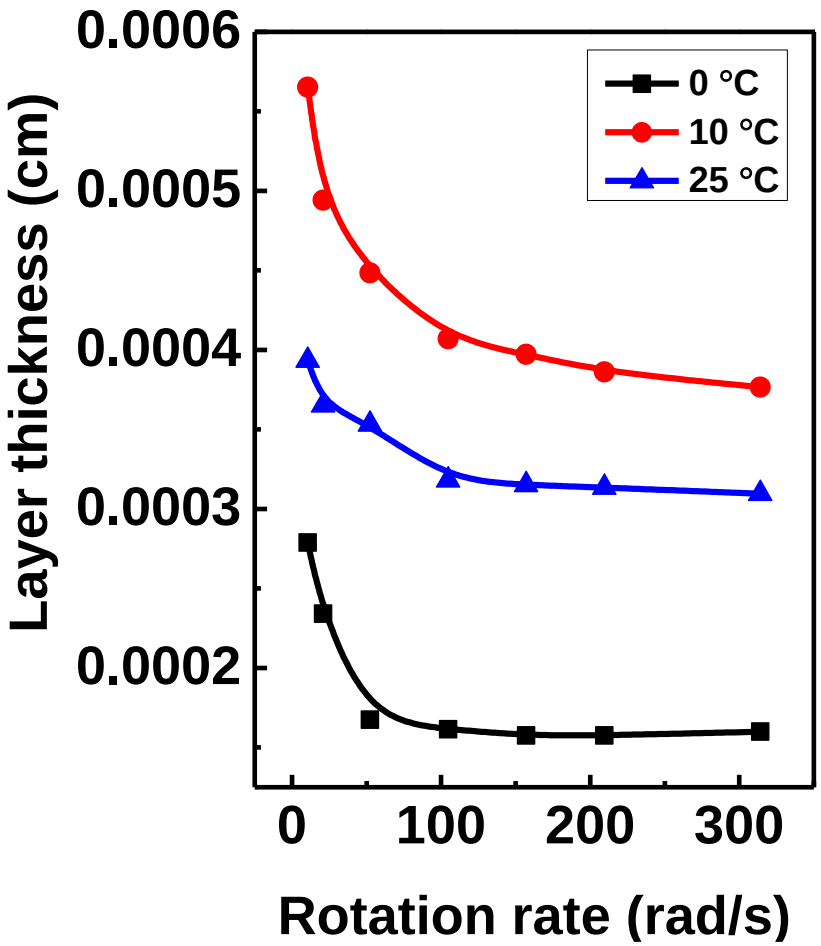

Figure 3. Diffusion layer thickness (δ) derived from the predicted transient current variation for $[Co(II)(CN)_5]^{3-}$ reduction at different rotation speeds and temperatures using Eqs. 1&3 (mentioned in the figure). Scan rate = 20 mV/s.

At the same time, the theoretically predicted concentration from the reduction current was not well matched with the experimentally observed Co(I) concentration (Fig.2 lines CB). In addition, the decreasing trend of the Co(I) concentration was irregular, i.e., 0 °C showed a high Co(I) concentration and 10 °C showed a lower concentration than 25 °C. The mismatch of the Co(I) concentration between the experimental and modelled values could be due to the data used for the theoretical model is reduction current, but the experimentally observed concentration is derived in solution in an ex-situ manner.

The difference transient current at low and high RPM may related to the diffusion layer thickness (δ). Fig.3 shows the δ $1.6x10^{-4}$ at 0 °C above ω = 50 (RPM curve a), which was increased to $4.0x10^{-4}$ cm at 10 °C (Fig.3 curve b). Further increases in temperature to 25 °C resulted in a slight decrease in δ value to $3.2x10^{-4}$ cm at above ω = 100 (RPM) (Fig.3 curve c). At high ω, the decrease in δ value is

known [26], but the decrease in δ at low temperatures may be due to the high concentration electrolyte i.e., a part of the diffusion layer act as solid.

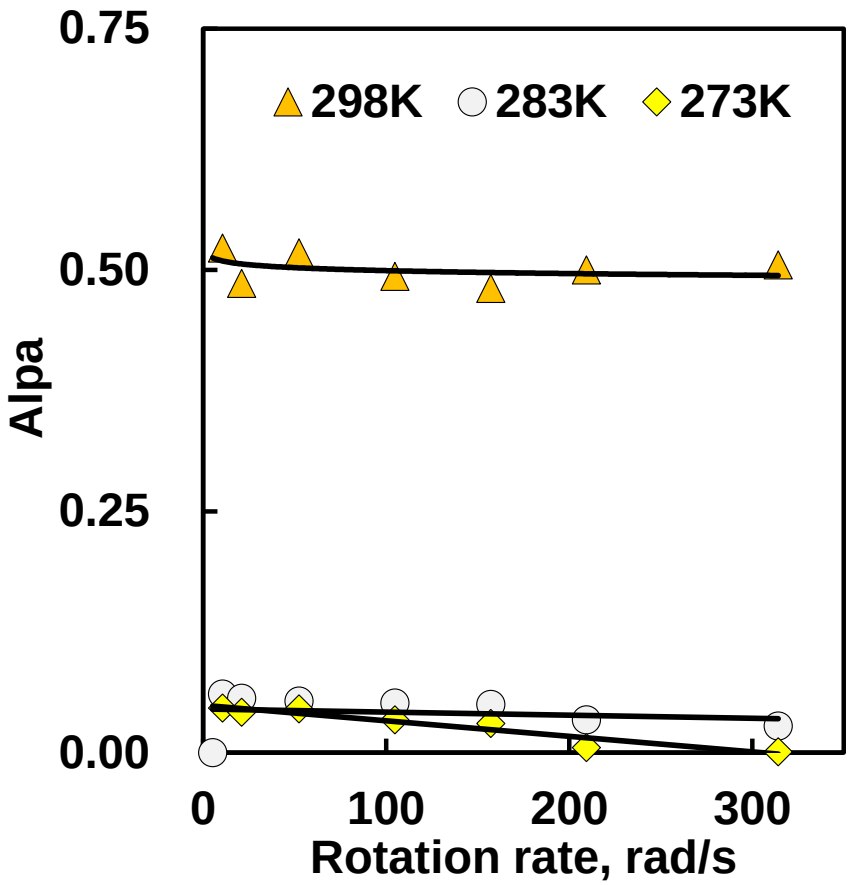

Figure 4. Transfer coefficient (α) derived from the predicted transient current variation for $[Co(II)(CN)_5]^{3-}$ reduction at different rotation speeds and temperatures using Eqs. 1&3 (mentioned in the figure). Scan rate = 20 mV/s.

The dimensionless transfer coefficient (α) determined using the Butler-Volmer equation was approximately zero at 0 °C and 10 °C (Fig.4 curve a &b). Normally, the α value changes from 0.3 to 0.7 [27], but a value below 0.3 suggests no change in the interfacial potential at low temperatures, meaning less energy is sufficient for electron transfer. At the same time, the α value was 0.5 at 25 °C (Fig.4 curve c), indicating a slight increase in interfacial potential that requires slightly higher energy for electron transfer.

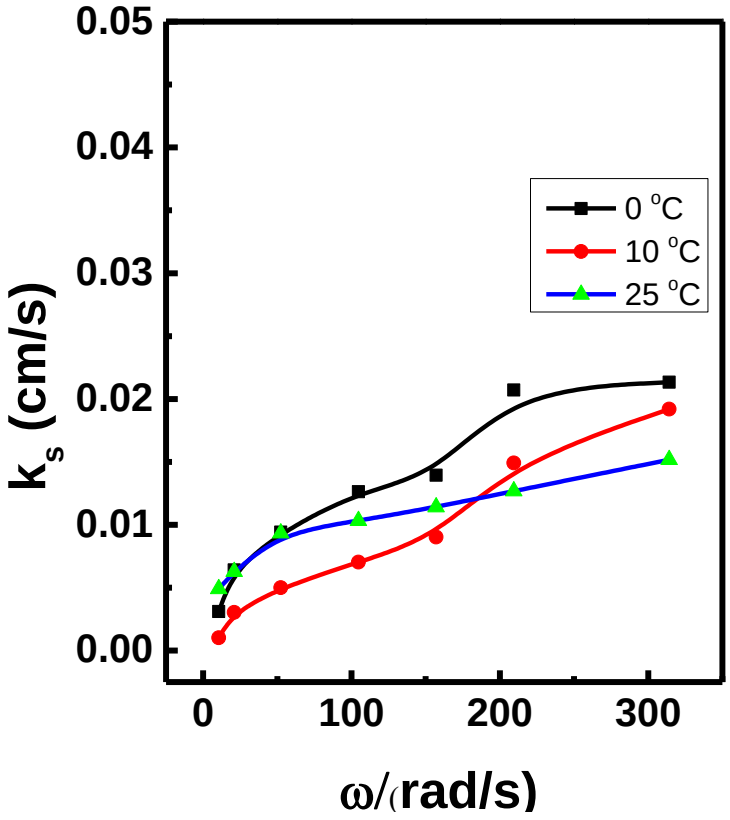

Figure 5. Heterogeneous electron transfer rate constant (k_s) derived from the predicted transient current variation for $[Co(II)(CN)_5]^{3-}$ reduction at different rotation speeds and temperatures using Eqs. 1&3 (mentioned in the figure). Scan rate = 20 mV/s.

Fig.5 shows the heterogeneous electrons transfer rate constant (k_s) for the Co(II) to Co(I) reduction current data using the Butler-Volmer equation (Eqn.7) digitally simulated for different temperatures and rotation rates. At high ω, the k_s values were higher at low temperatures (Fig.5 curve a), but the k_s value increased at high temperatures (Fig.5 curve c) at a low ω. The k_s values at a high ω at all temperatures were quasi-reversible [14]; here, Co(II) reduction follows a quasi-reversible electron transfer process. The average mass transfer coefficient (D_{ave}) predicted by the model equation in the form of dynamic diffusivity increased with temperature from 2.82×10^{-8} to 5.52×10^{-8} (cm^2/s), as shown in Fig. 6. Based on the slope of the average diffusion value at different temperatures (273–298 K), the activation energy (E_a) was approximately 18 kJ/mol, which is less when compare with the cobalt bipyridine complex in ionic liquid medium [28].

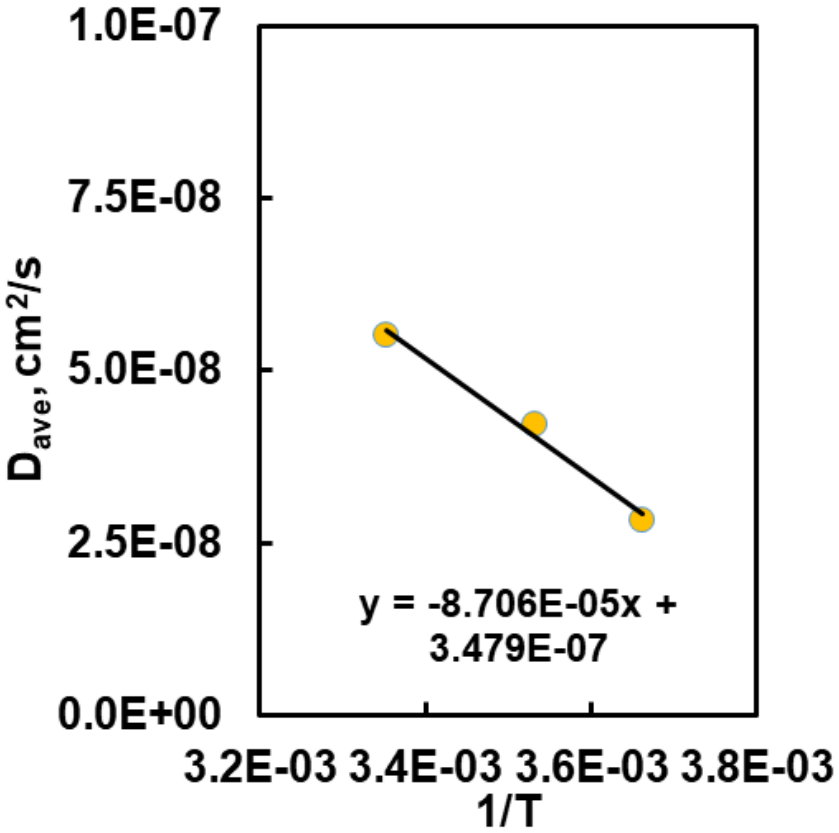

Figure 6. Average mass transfer coefficient (D_{ave}) derived from the predicted transient current variation for $[Co(II)(CN)_5]^{3-}$ reduction through different rotation speeds at different temperatures using eqs. 1&3 (mentioned in the figure). Scan rate = 20 mV/s.

4. CONCLUSIONS

A theoretical model for the transient reduction current for the E'reaction was validated with the experimental data for $[Co(II)(CN)_5]^{3-}$ reduction to $[Co(I)(CN)_5]^{4-}$ formation in a high concentration electrolyte during electrolysis. Through the developed theoretical collocation model, the predicted transient current for Co(II) reduction was well matched with the experimentally observed reduction current values for both rotation rates and temperatures. The theoretically predicted Co(I) concentration was not well matched to the experimentally observed concentration due to the experimentally observed concentration derived for the solution not by the reduction current. The transfer coefficient (α), diffusion layer thickness (δ), heterogeneous electron transfer (k_s), mass transfer coefficient in the form of dynamic diffusivity (D), and energy of activation were derived using the developed model for the E'reaction in high concentration electrolytes.

ACKNOWLEDGEMENT
This study was supported by the National Research Foundation of Korea (NRF) funded by Ministry of Engineering Science and Technology (MEST) from the Korean government (Grant No. NRF-2017R1A2A1A05001484).

References

1. T. Nguyen, R.F. Savinell, Flow Batteries, *Electrochem. Soc. Interface*, 19(3) (2010) 54-56.
2. C. Lamy, *Int. J. Hydrogen Energy,* 41(34) (2016) 15415-15425.
3. M. Govindan, A.M. Bond, I.-S. Moon, *Sci. Rep., UK*, 7(1) (2017) 29.
4. A. Wiebe, T. Gieshoff, S. Möhle, E. Rodrigo, M. Zirbes, S.R. Waldvogel, *Angew. Chem. Int. Edit*., 57(20) (2018) 5594-5619.
5. M. Skyllas-Kazacos, L. Cao, M. Kazacos, N. Kausar, A. Mousa, *ChemSusChem*, 9(13) (2016) 1521-1543.
6. P. Elumalai, H.N. Vasan, N. Munichandraiah, *J. Power Sources*, 93 (2001) 201-208.
7. J. Zheng, J.A. Lochala, A. Kwok, Z.D. Deng, J. Xiao, *Adv. Sci.*, 4(8) (2017) 1700032.
8. M. Ulaganathan, V. Aravindan, Q. Yan, S. Madhavi, M. Skyllas-Kazacos, T.M. Lim, *Adv. Mater. Interfaces*, 3(1) (2016) 1500309.
9. P. Polczynski, R. Jurczakowski, W. Grochala, J. Phys. Chem. C, 117(40) (2013) 20689-20696.
10. M. Govindan, S.-J. Chung, I.-S. Moon, *Ind. Eng. Chem. Res.*, 51(6) (2012) 2697-2703.
11. J. Hanzlik, A.A. Vlcek, *J. Chem. Soc. Chem. Comm*., (2) (1969) 47-48.
12. G. Muthuraman, I.S. Moon, *J. Hazard. Mater*., 325 (2017) 157-162.
13. D. Pletcher, A. Heather Thompson, *J. Chem. Soc., Faraday Trans.*, 93 (1997) 3669-3675.
14. J. Strutwolf, W.W. Schoeller, *Electroanalysis*, 8(11) (1996) 1034-1039.
15. Y.-F. Wu, C.-H. Chen, *J. Electrochem. Soc*., 161(8) (2014) E3276-E3282.
16. C. Deslouis, B. Tribollet, M. Duprat, F. Moran, *J. Electrochem. Soc.*, 134(10) (1987) 2496-2501.
17. P.H.M. Leal, N.A. Leite, P.R.P. Viana, F.V.V. de Sousa, O.E. Barcia, O.R. Mattos, *J. Electrochem. Soc.*, 165(9) (2018) H466-H472.
18. B. Speiser, *J. Electroanal. Chem.*, 413(1) (1996) 67-79.
19. A. J. Bard and L. R. Faulkner, *Electrochemical Methods. Fundamentals and Applications*, John Wiley & Sons (2001).
20. J. Villadsen, W. Stewart, *Chem. Eng. Sci.*, 22 (1967) 1483–1501.
21. P.N. Brown, G.D. Byrne, A.C. Hindmarsh, *SIAM J. Sci. Statist. Comput.*, 10 (1989) 1038–1051.
22. W.G. Shim, K. He, S. Gray, I.S. Moon, *Sep. Purif. Technol.*, 143 (2015) 94–104.
23. J.A. Nelder, R. *Mead, Comput. J.*, 7 (1965) 308–313.
24. A.W. Adamson, *J. Am. Chem. Soc.*, 73(12) (1951) 5710-5713.
25. C. Comninellis, E. Plattner, P. Javet, *J. Appl. Electrochem*., 9(5) (1979) 595-601.
26. J. O'M. Bockris and A. K. N. Reddy, *Modern Electrochemistry*, Vol. 2, MacDonald, London (1970) p. 1058.
27. J.M Saveant, D. Tessier, *Faraday Disc, Chem. Soc.*, 74 (57) (1982) 1a, p. 71.
28. Y. Katayama, S. Nakayama, N. Tachikawa, K. Yoshii, *J. Electrochem. Soc.*, 164 (2017) H5286.

© 2020 The Authors. Published by ESG (www.electrochemsci.org). This article is an open access article distributed under the terms and conditions of the Creative Commons Attribution license (http://creativecommons.org/licenses/by/4.0/).